Advances in Environmental Technology 12(2) 2026, 220-231.

Iranian Reasearch Organization for Science and Technology (IROST)

Advances in Environmental Technology

Journal home page: https://aet.irost.ir

Enhanced arsenic (V) removal from water using aluminium oxide nanoparticle-incorporated Polyethersulfone hollow fiber membranes

Mruthyunjaya Swamy Dasaiah[a], Arun M. Isloor[a]*, Muttanna Venkatesh[a], Vijayendra Shetti[b]

[a] *Membrane and Separation Technology Laboratory, Department of Chemistry, National Institute of Technology Karnataka, Surathkal, India.*

[b] *Department of Chemistry, National Institute of Technology Karnataka, Surathkal, India.*

ARTICLE INFO

Document Type:
Research Paper

Article history:
Received 02 October 2025
Received in revised form
21 April 2026
Accepted 21 April 2026

Keywords:
Hollow fiber membranes
Ultrafiltration
Flux
Rejection
Nanoparticles
Arsenic contamination
Wastewater

ABSTRACT

The expansion of urbanization, industrialization, and population has led to water pollution due to severe contamination by toxic pollutants, increasing the demand for pure water. Arsenic poisoning of water is considered a highly hazardous chemical poisoning due to its harmful effects on the environment and human health. The present study combines nanotechnology and membrane technology to overcome water scarcity issues and the removal of arsenic from contaminated water. Polyethersulfone (PES) hollow fiber membranes, with and without nanoparticles (NPs), were fabricated through the dry-wet spinning process and used for ultrafiltration studies. Physicochemical characterization confirmed the successful synthesis of bare nanoparticles, and further, membranes were characterized and analyzed by various studies. The study demonstrated significant improvements in As (V) removal efficiency and water flux. The optimized membrane achieved a removal rate of 79.23% and the highest flux of 26.7 L/m²/h compared to the pristine membrane, which had a 65% removal rate and a flux of 18 L/m²/h, emphasizing potential for water purification applications.

1. Introduction

High levels of arsenic (V) in drinking water pose a significant health threat to approximately ten million people in low-income countries. This contamination is widely regarded as the worst chemical poisoning crisis worldwide at present. Nonetheless, numerous chemical forms of arsenic differ greatly in terms of solubility, toxicity, and bioavailability. Inorganic arsenic compounds are known carcinogens [1].

Epidemiological studies in humans have shown a clear association between As (V) exposure and the development of cancer affecting the skin, respiratory organs, and urinary bladder. Its specific chemical form and solubility influence the harmful effects of arsenic and its absorption capacity. Additionally, its toxicity is significantly impacted by the metabolic processes it undergoes, particularly

*Corresponding author Tel.: +91 944 8523990
E-mail: isloor@yahoo.com
DOI: 10.22104/aet.2026.7907.2213

the conversion to a trivalent state and the oxidative methylation that leads to a pentavalent form [2,3]. The poisonous qualities of trivalent arsenicals, particularly methylated ones, are stronger than those of pentavalent arsenicals. The exact mechanism by which arsenic acts remain unclear, although several theories have been proposed. Biochemically, pentavalent inorganic arsenic can replace phosphate in various processes. In its trivalent form, both organic (methylated) and inorganic arsenic can react with essential protein thiols to prevent them from functioning [4]. Potential pathways associated with cancer include genotoxicity, changes in deoxyribonucleic acid (DNA) methylation, oxidative stress, modifications in cellular expansion, synergistic cancer development, and the promotion of tumours.

Numerous methods for decontaminating arsenic have been described by researchers worldwide. These include membrane filtration using reverse osmosis and nanofiltration, as well as coagulation, oxidation, flocculation, phytoremediation, and adsorption. Many of these techniques have drawbacks, such as precipitation, which can produce a lot of hazardous sludge and seriously harm the environment. To effectively retain arsenic, an ion exchange mechanism is utilized. However, the efficiency of this ion exchange process is significantly limited due to its poor selectivity for As(V), which is influenced by strong competition from various co-existing anions. Consequently, the ultrafiltration membrane technique has emerged as a promising method for separating different heavy metals, especially the hazardous arsenic ions. To separate different types of toxic metals, the ultrafiltration membrane technique [5] is becoming more and more significant. High retention permeability and cost-effectiveness are two benefits of the ultrafiltration process [6]. In this study, Polyethersulfone served as the primary polymer for creating hollow fiber membranes (HFMs) [7]. PES is a type of engineering thermoplastic valued for its excellent properties, such as high Tg and excellent thermooxidative stability. Over the past decade, there has been a growing focus on arsenic exposure in the development of new organic–inorganic composite membranes with tailored features. These membranes have been effectively used in techniques like gas separation, pervaporation, and nano- and ultrafiltration, leading to significant advancements [8].

Recently, NPs infused polymeric membranes have been utilized in the membrane water filtration process, including titanium oxide (TiO_2), silica, zirconium dioxide (ZrO_2), and aluminium oxide (Al_2O_3) [7]. Other inorganic salts, such as lithium salts, have been combined with polyvinylidene fluoride (PVDF), polyphenylsulfone (PPSU), cellulose acetate (CA), polysulfone (PSF/PSU), Polyetherimide (PEI), etc. Due to their excellent decontamination efficiency and inexpensive manufacturing costs, iron and aluminium-based nano adsorbents [8] have been widely used among nanomaterials. Additionally, the United Nations Environment Programme (UNEP) has recommended that the most effective technology for removing arsenic from water is alumina-based adsorption [9].

According to previous literature studies, the performance of NPs in water purification was significantly improved when they were incorporated into polymeric membranes. Nanocomposite ultrafiltration and nanofiltration membranes have also been reported to integrate adsorption, hydrophilicity, antifouling ability, and photocatalytic properties. However, most of these studies have focused on flat-sheet or electrospun membranes [10]. On the other hand, Talukder et al. developed ZrO_2 NPs incorporated PPSU/CA polymeric membranes for water arsenic removal studies. These membranes exhibited an arsenic removal efficacy of about 87.24% and a permeability of 89.94 L m^{-2} bar^{-1} [11]. Kumar et al. developed ZnO-MgO NPs incepted PPSU/CA membranes, which exhibited 81.31 and 78.48% of arsenic rejection, along with 69.58 and 198.47 L m^{-2} h^{-1} bar^{-1}, respectively, at 0.6 wt% loading [12]. Zr-based NPs incorporated into PSU HFM achieved improved flux due to hydrophilicity and porosity. He et al. observed a high removal efficacy with an excellent arsenate adsorption capacity of 131.7 mg/g [13]. ZnO NPs embedded CA membranes demonstrated the favorable flux and rejection balance, achieving 58.77% arsenic removal efficacy at 1000 mg/L feed load [14]. The studies mentioned above examined flat sheet, hollow fiber, and blend membranes that incorporated various

single or binary oxide nanoparticles for arsenic removal from wastewater. Most of the existing literature emphasizes achieving high permeability with moderate rejection rates of 58 to 87% using PPSU and PSU membranes. However, there is a noticeable lack of systematic research specifically on PES hollow fiber membranes embedded with Al_2O_3 for As(V) removal. Although many membrane technologies are increasingly used for water treatment, traditional membranes often face issues related to hydrophilicity, flux, and arsenic removal efficiency. Different modification strategies have been explored, but these often compromise membrane stability, leading to inconsistent distribution of nanoparticles.

There is a clear need to develop membranes that can simultaneously enhance water flux and selective arsenic removal without adding fabrication complexity or cost, especially through ultrafiltration. This leverages the natural affinity of Al_2O_3 nanoparticles for arsenic (As(V)), improving arsenic removal from water. To address this, Al_2O_3 NPs-embedded PES HFMs have shown improvements in As(V) removal, water uptake, contact angle, morphology, topography, and porosity, with moderate flux performance. This research provides a comprehensive understanding of the impact of nanoparticle integration on membrane performance and offers a promising pathway for next-generation membrane-based water treatment solutions.

2. Materials and methods

2.1. Materials

Polyethersulphone (PES) was obtained from the Solvay Company, Belgium. Glycerol was sourced from Pallav's Chemical Pvt Ltd.

Polyvinylpyrrolidone (PVP K17), N-methyl-2-pyrrolidone (NMP), aluminium oxide nanoparticles (Al_2O_3 NPs), and a standard arsenic V solution (1000 mg/ml) were acquired from Sigma Aldrich India.

2.2. Methods

2.2.1. Fabrication of HFMs

The dry-wet process and phase inversion technique were used to fabricate PES HFMs with or without NPs [15] via the nonsolvent-induced phase inversion (NIPS) process. Before fabrication, the polymer was dried for 24 hours at 60°C to remove the moisture content in PES. Initially, with and without NPs incorporated, the PVP containing NMP solution was sonicated for 30 minutes separately based on the compositions listed in Table 1. To the above solution, a specified amount of PES was added, and the mixture was then stirred with an overhead stirrer for 24 hours at 60 °C to produce a homogenous dope matrix [16,17]. The dope solution that had been earlier prepared was utilized while spinning. Initially, the dope solution was passed into the annular region of the spinneret using a gear pump in an inert nitrogen atmosphere. Subsequently, the bore liquid was Milli-Q water sent through the spinneret's inner lumen. To maintain the proper phase inversion, the spinneret was placed at a specific distance from the water (non-solvent) bath to create the membrane using the dry-wet approach [18]. Finally, all membranes were immersed in water for 24h to remove residual solvent and soaked in a 20% glycerol solution to reduce pore collapse during filtration. After post-treatment, all membranes were dried at room temperature (RT) and further utilized for various performance studies [19]. The parameters that followed during the fabrication process were maintained based on Table 2. The schematic representation of the HFMs reflecting production was shown in Figure 1.

2.3. Characterizations of the NPs and the HF membranes

The physicochemical characteristics of NPs were assessed using various analytical techniques. Thermogravimetric analysis (TGA) provided insights into their thermal stability.

Table 1. Composition of the membrane dope.

Type of Membrane	PES (g)	NMP (g)	PVP (g)	NPs
M - 0	22	73	5	0
M - 1	22	73	5	0.25
M - 2	22	73	5	0.50
M - 3	22	73	5	0.75

Table 2. Spinning parameters.

Parameters	Condition
Spinneret OD/ID (mm)	1.1/0.55
Dope solution	PES/Al_2O_3/PVP/NMP
Bore fluid, coagulation, and rinsing bath	H_2O
Bore fluid flow rate (mL/min)	5
Air gap (cm)	5
Coagulation and rinsing bath (°C)	27

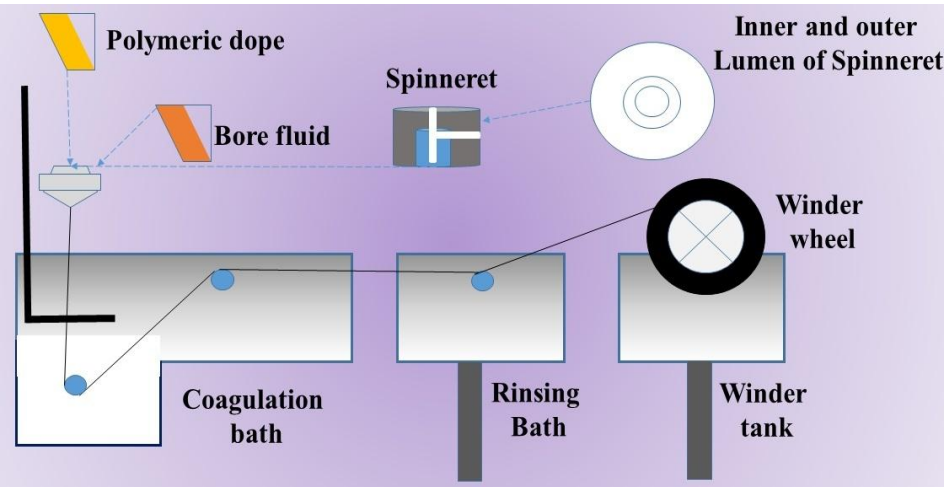

Fig. 1. Schematic representation of the HFM fabrication system [20].

The zeta potential and particle size analysis were employed to determine surface charge and the average particle size distribution (Litesizer model TM500 from Anton Paar, Austria). The morphology of both the nanoparticles and membranes was examined using scanning electron microscopy (SEM) with a Jeol JSM-6380LA model. The NPs' chemical composition and mapping were carried out using energy dispersive X-ray spectroscopy (EDAX). Before SEM analysis, the membrane samples were freeze-fractured with liquid nitrogen and coated with gold. Additionally, Fourier-transform infrared spectroscopy (FTIR) was used to identify characteristic peaks associated with the functional groups in Al_2O_3, and membrane roughness parameters were carried out using atomic force microscopy (Flex-Axiom AFM, M/s Nanosurf, Switzerland).

2.4. Membrane performance studies

2.4.1. Flux studies of HFMs

The pure water Flux (PWF, indicated with *'J'*) was examined using the ultrafiltration cross-flow model [21]. Five suitable membrane samples, each measuring 15 cm in length, were taken from the group of membranes [22].

Once the potting process (with an epoxy-to-hardener ratio of 2:1) was completed, a compaction pressure of 2.5 bar was applied for 30 minutes to facilitate the flow of Milli-Q water through the membranes.

Transmembrane pressure (TMP) was subsequently reduced to one bar, and the volume of water and flux were calculated every ten minutes using Equation 1.

$$J = \frac{Q}{n\pi L \Delta P D_i} \quad (1)$$

where *'n'* is the number of HFMs, *'D_i'* is the Spinneret inner diameter, *'ΔP'* is – TMP, 'Q' is- Volume flow rate (mL/h), and *'L'* is- HFM length.

2.4.2. Hydrophilicity and Wettability

The wettability of the HFMs was assessed via water uptake (WU) based on the dry and wet weight of the membranes and calculated using Equation 2; the hydrophilicity of the membranes was understood by water contact angle (WCA) [the FTA 200 contact angle analyzer through the sessile drop method] examinations, with additional confirmation offered by PWF.

$$\% \text{ Water Uptake} = \frac{(Ww - Wd)}{Ww} \times 100 \quad (2)$$

where 'W_w' and 'W_d' are the wet and dry weights of the HFMs, respectively.

2.4.3. Removal of arsenic by HFMs

An analysis of As (V) retention was conducted on drinking water contaminated with arsenic, utilizing both pristine membranes and those infused with nano-Al_2O_3. The concentration of As (V) in the contaminated water was measured using atomic absorption spectroscopy (AAS) with a Perkin-Elmer device. A laboratory-produced solution containing 1 mg/L of arsenic, with a pH of 6.9 ± 0.2, served as the feed '(C_f)' for arsenic filtration. The solution was then subjected to the UF cross-flow method while maintaining a TMP of 2 bar. The permeate '(C_p)' of each membrane was recorded, and the percentage of arsenic rejection was calculated through the varied concentration of 'C_f', and 'C_p' based on Equation 3.

$$\% R = \left(1 - \frac{C_p}{C_f}\right) \times 100 \quad (3)$$

3. Results and discussion

3.1. Functional groups identification

Al_2O_3 NPs were analyzed using FTIR, and it revealed a broad characteristic peak at 3465 cm^{-1} that was attributed to the -OH stretching vibrations associated with the water molecule in the lattice; this could suggest that there was moisture present in the KBr powder. There was also a weak peak observed at 1636 cm^{-1}, which was linked to the stretching vibrations of the Al-OH bond. Additionally, a peak at 756 cm^{-1} corresponded to the symmetric stretching vibration of the Al-O-Al bond [23], as illustrated in Figure 2.

3.2. Thermogravimetric analysis

In Figure 2, the Al_2O_3 NPs thermogram from thermogravimetric analysis reveals two main areas of mass loss. The first gradual mass loss occurred up to about 136°C and was produced by the evaporation of physiosorbed water. The second mass loss was observed around 280°C due to Dihydroxylation, brought on by the breakage of Al-OH bonds [24].

3.3. Particle size and zeta potential of aluminium oxide nanoparticles

Zeta or α-potential is a parameter that measures the potential difference between the dispersion medium and the stationary layer on the dispersed particle and the surface charge of the material [25]. By examining the zeta potential value, one can forecast the particle's stability in a solution, either in the short or long term. Because the repulsion between the particles keeps them apart and prevents them from sticking together and precipitating out, a particle with a high positive or negative zeta-potential value will be able to remain stable as a dispersion. Zeta potential analysis revealed the surface charge of aluminium oxide nanoparticles, +14.4 mV at neutral pH. The nanoparticle showed an average particle size of 314 nm, whereas the hydrodynamic diameter was observed to be 405 nm, signifying the hydrophilicity of nano-alumina [26], as shown in Figure 2.

3.4. Surface morphology of Al_2O_3 nanoparticle

The analysis of the surface structure and elemental makeup of Al_2O_3 nanoparticles was performed using SEM and EDS. The results showed a clustered and irregular topography, suggesting a rough surface texture [27]. This roughness improved hydrophilicity, contact angle, water absorption, and permeability. The morphology of the NPs significantly affected water flux, increased surface area, and enhanced porosity, all of which contributed to the reduced resistance to water flow. Optimizing their incorporation into the membrane matrix boosted their rejection effectiveness, while the EDS spectrum verified the presence of aluminium and oxygen, highlighted by distinct peaks at their respective electron volt [28]. The clear identification of the aluminium peak corroborates the structural improvement in both the membrane matrix and the NPs, as shown in Figure 3.

3.5. Morphology of the membranes

Figure 4 shows the cross-sectional images of the fabricated HFMs with and without the incorporation of Al_2O_3 NPs. The membrane displays an asymmetric structure, with a dense top or skin layer, which is responsible for rejection (selectivity) and permeability.

Beneath the skin layer is the sublayer with a spongy macro void structure with finger-like projections, which act as support to the above skin layer, providing it with mechanical strength. In Figure 4., the M-2 membrane displays a very distinct skin layer compared to other membranes, which is responsible for the higher rejection of arsenic ions[29].

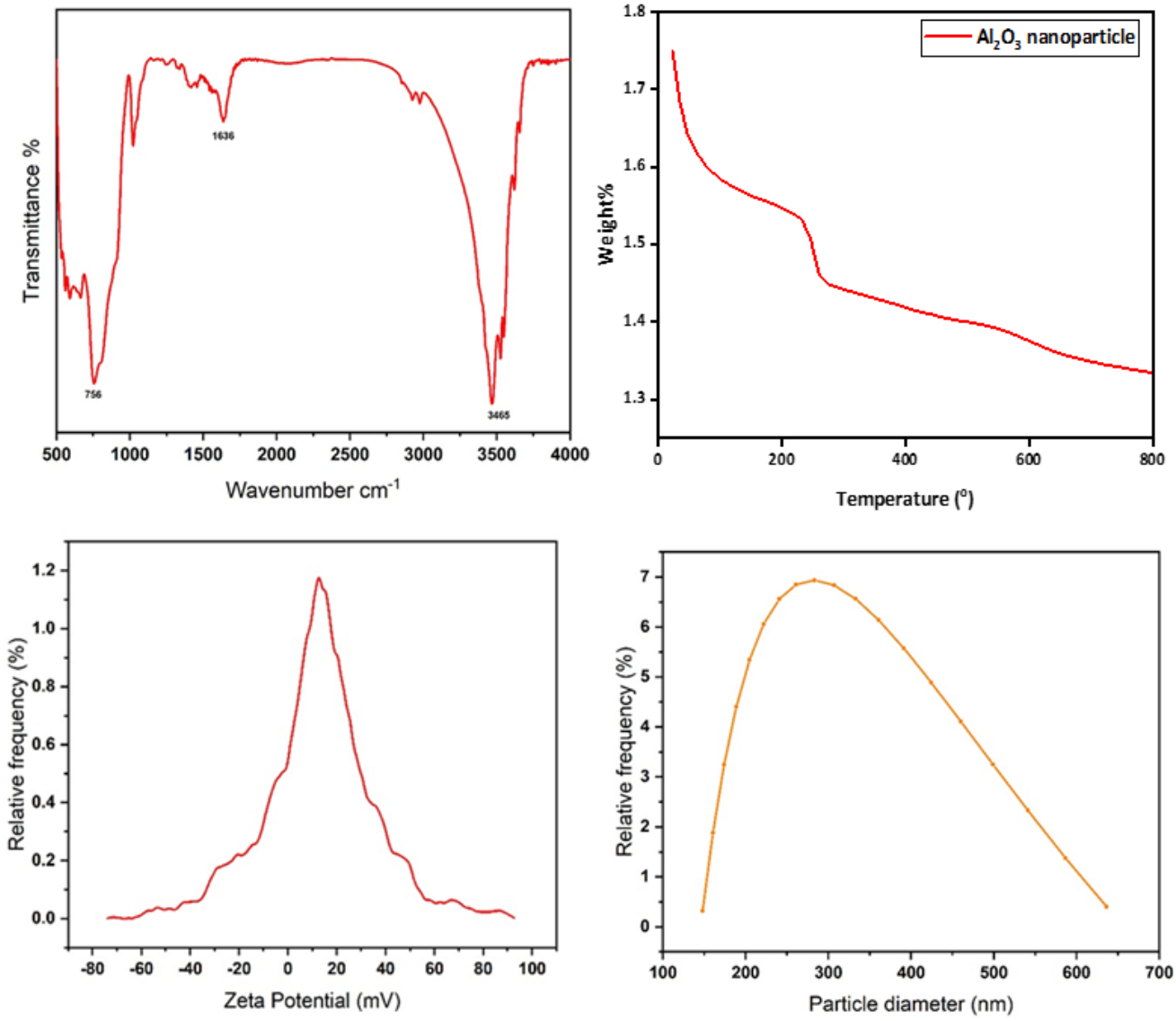

Fig. 2. FTIR, TGA, Zeta potential, and particle size distribution of Al_2O_3 nanoparticles.

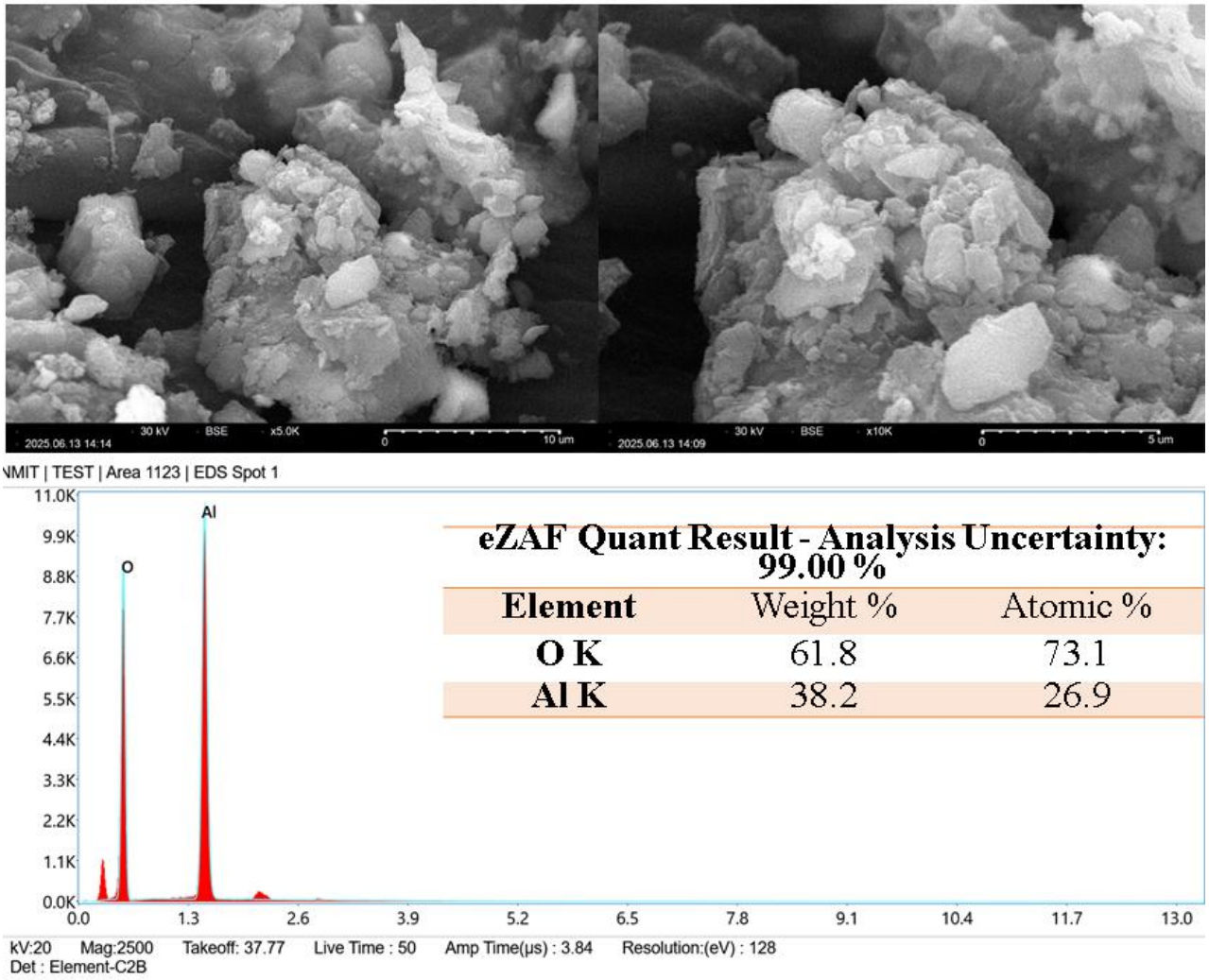

Fig. 3. SEM and EDS of Al_2O_3 NPs.

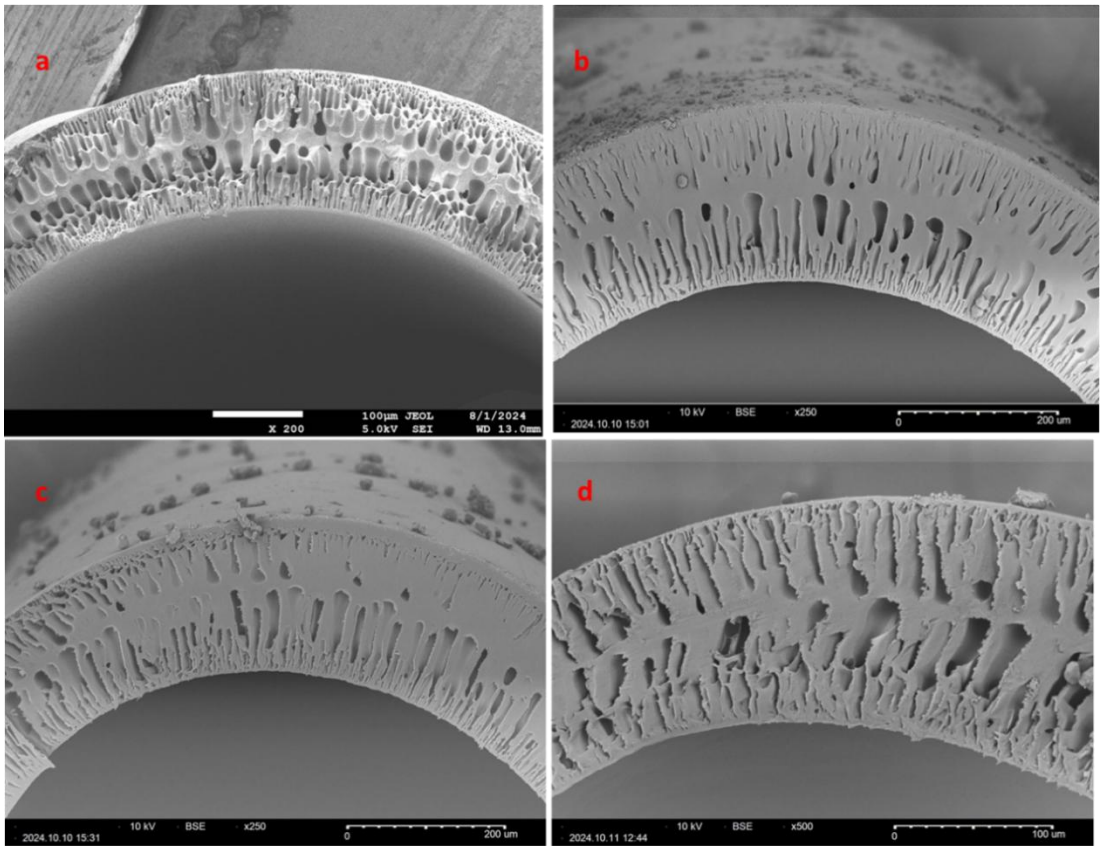

Fig. 4. SEM of HFMs: (a) M-0, b) M-1, c) M-2, and d) M-3.

3.6. Atomic force microscopy (AFM)

The surface roughness of the HFMs, with or without an additive, was examined using AFM studies, as described in Figure 5. It reveals that the M-2 membrane exhibits a relatively smoother surface compared to the NPs incorporated membranes. The roughness parameters of the respective membranes are illustrated in Table 3. The reduction in roughness after incorporating NPs is beneficial for significantly improving membrane performance[30]. A smoother membrane surface correlated with better water flux. This morphological refinement enhances long-term operational stability, particularly in the removal of specific pollutants from water. It demonstrates excellent arsenic removal efficiency due to increased hydrophilicity. The interaction of nanoparticles (NPs) influences not only topographical roughness but also interacts with sites through chemical reactions with pollutants[31,32]. Consequently, AFM indicates that the incorporation of NPs modulates surface roughness and optimizes surface chemistry to achieve a balance between flux and efficiency.

3.7. Pure water flux

The quantity of water flowing through the membrane per unit area per time is termed flux through the membrane, which was measured using a tight ultrafiltration cross-flow method.

A pure water flux of 18.12 LMH was observed for the M-0 membrane. As the nano-alumina incorporation in the polymeric dope was raised, the PWF increased. The optimized membrane M-2 showed a pure water flux of 26.79 LMH. The increase in flux may be attributed to the hydrophilic nature of the incorporated Al_2O_3 nanoparticle [33,34]. When the loading increases above 50 mg, alumina nanoparticles are found to agglomerate, leading to reduced flux values, as shown in Figure 6. In this case, after incorporating Al_2O_3 NPs, the flux increased significantly compared to the pristine membranes. However, the absolute flux is lower than in typical ultrafiltration studies, owing to tight ultrafiltration at 2 bar transmembrane pressure. This study,

therefore, prioritizes contaminant removal performance and highlights the balance achieved between the membranes' selectivity and permeability.

3.8. Contact angle

Figure 7 demonstrates the hydrophilicity of the HFMs' surface through contact angle measurements, which reveal improved wettability. This characteristic significantly influences water flux.

Table 3. Surface roughness of HFMs.

Membranes	RMS roughness (S_q) nm	Mean roughness (S_a) nm
M-2	73.39	56.12
M-N	111.6	87.6

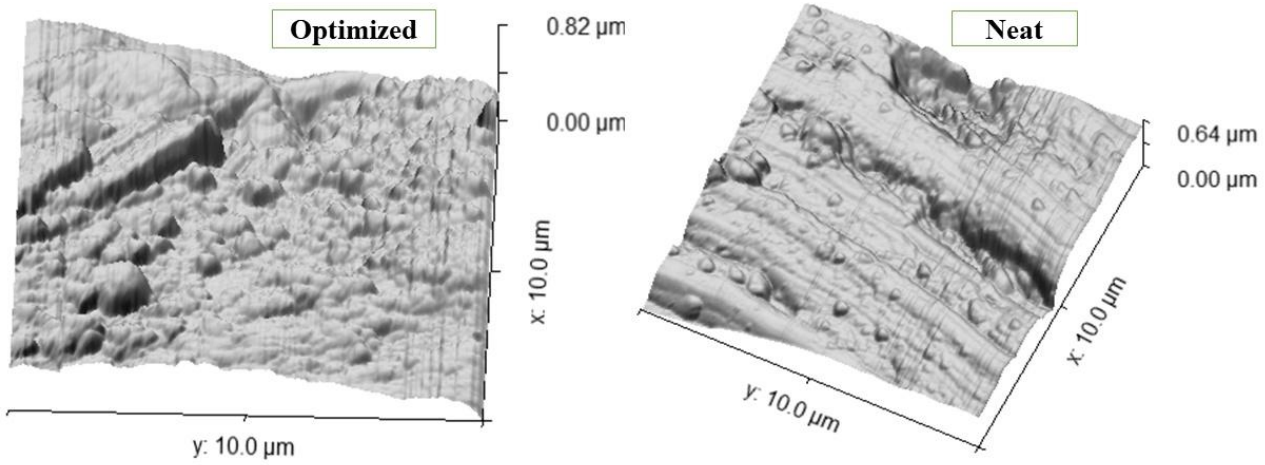

Fig. 5. AFM of Neat and M-2 membranes.

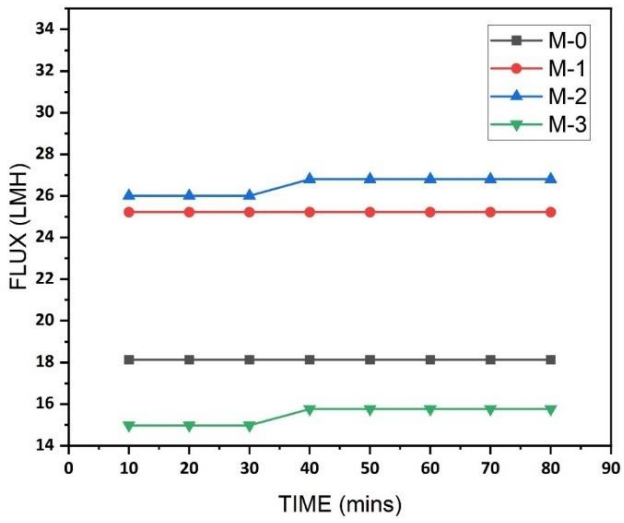

Fig. 6. Pure water flux studies of the neat and modified membranes.

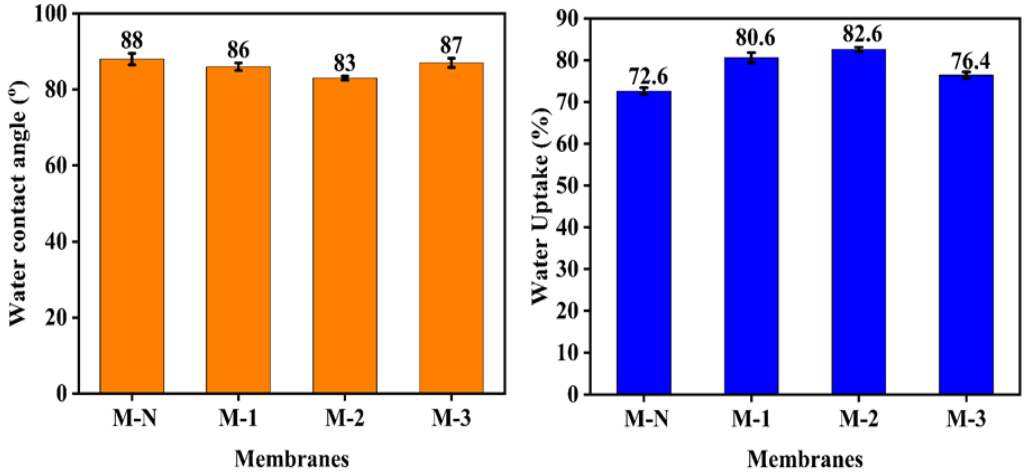

Fig. 7. Water contact angle (WCA) and Water uptake (WU) of all membranes.

The NPs infused membranes showed a reduced WCA compared with M-0 membranes, indicating a higher degree of hydrophilicity. Whereas M-0, M-1, and M-2 were 88°, 86°, and 83°, respectively. However, for the M-3 (87°) membrane, there was a slight increase in contact angle differences, likely due to the clustering of nanoparticles (NPs) and their visibility on the membrane's surface. Properly optimizing the incorporation of NPs enhanced both the functional performance and the wettability of the membrane surface [35].

3.9. Water uptake

First, each membrane was cut into 2 cm lengths and immersed in water for 24 hr., and then weighed and kept for drying at 60 °C using a hot air oven, and the dried membranes are weighed [36]. Finally, water uptake was calculated using Equation 2. The WU capability of the HFMs is a critical parameter of their hydrophilicity, which directly influences water flux and fouling resistance. As depicted in Figure 7, the pristine membrane exhibited a water uptake of 72.6%, while the membrane incorporated with Al_2O_3 NPs demonstrated improved water uptake percentages of 80.6% (M-1), 82.4% (M-2), and 76.4% (M-3), respectively. The M-2 reached the highest water uptake, suggesting that the optimal concentration of NPs leads to the highest hydrophilic nature of the PES matrix. This results in better water flux and excellent rejection efficacy. In contrast, M-3 showed a reduction in the water uptake, which led to agglomeration at higher loadings, potentially leading to pore blockages and uneven dispersion within the membranes.

3.10. Arsenic decontamination studies

1 mg/L concentration of sodium arsenate was tested using membranes with different compositions of alumina nanoparticles.

Al_2O_3 is positively charged at neutral pH, as revealed by the zeta potential analysis. Therefore, when arsenic solution passes through membranes containing alumina, it is electrostatically attracted to the positively charged nanoparticles.

In this study, the UF membranes had nanoparticles embedded within the PES matrix, providing additional adsorption sites beyond the size exclusion of the membranes. Arsenate ions adsorb onto the modified membrane surfaces, thus increasing rejection efficiency.

This dual mechanism sieving via tight ultrafiltration and chemical adsorption by aluminum oxide nanoparticles demonstrated improved rejection performance compared to unmodified membranes [37,38].

However, alumina's intrinsic property is such that its zeta potential can become negative in basic pH, which can further enhance rejection due to electrostatic repulsion caused by the alumina nanoparticles on arsenate ions [39].

A membrane without nanoparticles showed a 65.2% rejection of arsenate ions, possibly due to electrostatic repulsion from the $-SO_2$ groups in the PES backbone.

As the nanoparticle content in the membrane increased, higher rejection rates were observed,

reaching a maximum of 79.23% with the M-2 membrane, as shown in Figure 8 and compared with previous literature studies mentioned in Table 4.

Nonetheless, higher nanoparticle loadings may lead to agglomeration, reducing arsenic removal efficiency. Additionally, arsenic (V) adsorbs onto Al_2O_3 via coordination between its oxygen atoms. This reaction depends on ambient conditions, such as basic, acidic, dissociative, or non-dissociative environments.

3.11. Stability of the Nano hybrid and membrane reusability

Throughout these experiments, the Al_2O_3 Nano hybrid material demonstrated notable stability, with no significant leaching detected over extended periods of up to 48 hours. The adsorption capacity and rejection efficiency exhibited only slight variations, confirming the robustness of the Nano hybrid within the polymer matrix. For reusability assessments, the membranes underwent three cycles of adsorption and desorption using an alkaline NaOH solution at pH 10. The arsenic rejection efficiency remained above 75% after these cycles, indicating excellent reusability and mechanical integrity of the mixed matrix membrane (MMM) hollow fiber membrane (HFM).

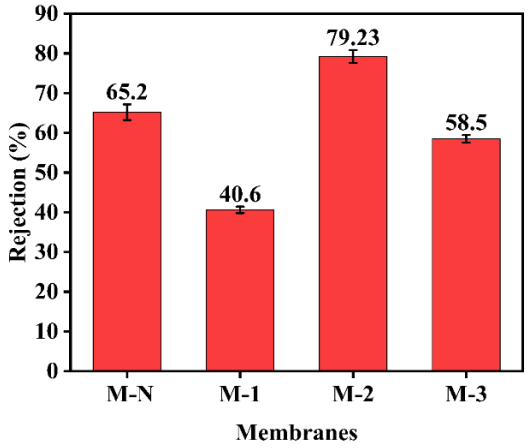

Fig. 8. Arsenic rejection studies through the pristine and modified membranes.

Table 4. Comparison with previous literature studies.

Material or Membranes type	Rejection efficacy (%)	Flux (L m^{-2} h^{-1})	References
CA/ZnO	58.77	5-25% increment by increasing pressure	[14]
PSU/ZnO	71	13	[10]
PES/Kaolin	30	-	[40]
Al_2O_3/TiO_2	99.9%	-	[38]
ZnO-MgO@PPSU/CA	81.31	198	[12]
PES/Al_2O_3 HFM	79.23	26.7	This work

4. Conclusion

This work highlighted the critical issues associated with health risks posed by arsenic, mainly focusing on their effects on human health and ecosystems. The investigation demonstrated the effective use of PES HFMs infused with Al_2O_3 NPs to improve arsenic removal capabilities. The significant increase in both the arsenic rejection rate to 79.23% and PWF to 26.79 L m^{-2} h^{-1} underscores the potential of these membranes for water purification applications. This advancement addresses the pressing concerns of arsenic contamination. Looking ahead, there is considerable potential for further research and development in this area. Future studies could explore the scalability of the membrane fabrication process, aiming to produce large quantities while maintaining performance efficiency. Additionally, investigating the incorporation of other inorganic additives alongside nano-alumina could lead to even more effective membrane properties,

enhancing the removal capabilities for a wider range of contaminants. Moreover, as we better understand the interactions between membrane materials and various heavy metals, it could be beneficial to conduct long-term field studies to assess the real-world applicability and durability of these membranes. Expanding research to evaluate the economic viability of using these advanced membranes in various industrial and municipal water treatment facilities could also prove advantageous. Ultimately, the goal is to create sustainable solutions that not only improve water quality but also protect public health and the integrity of ecosystems affected by heavy metal pollution.

Abbreviations

AFM	Atomic force microscopy
CA	Cellulose acetate
EDS	Energy dispersive X-ray spectroscopy
FTIR	Fourier transform infrared spectroscopy
HFMs	Hollow fiber membranes
MIM	2-methylimidazole
NIPs	Non-solvent-induced phase separation
NMP	N-methyl-2-pyrrolidone
NPs	Nanoparticles
PEI	Polyetherimide
PES	Polyethersulfone
PPSU	Polyphenylsulfone
PS	Particle size
PVP	Polyvinylpyrrolidone
PWF	Pure water flux
RT	Room temperature
SEM	Scanning electron microscope
TGA	Thermogravimetric analysis
TMP	Transmembrane pressure
UF	Ultrafiltration
WCA	Water contact angle
WU	Water uptake
ZP	Zeta potential

Acknowledgements

The authors express their gratitude to the National Institute of Technology (NIT) Surathkal in Karnataka, India, for offering instrumental, infrastructural, and laboratory support. Additionally, authors extend their thanks to the Central Research Facility at NIT Karnataka and the Bhabha Atomic Research Centre BARC Tarapur, Maharashtra, India.

Author's contribution

Mruthyunjaya Swamy D.: Investigation, Methodology, Data curation, Formal analysis, Writing – original draft, Lab experiments. Muttanna Venkatesh: Investigation, Data curation, Validation, Characterization. Arun M. Isloor: Conceptualization, Supervision, Project administration, Methodology, Writing – review & editing. Vijayendra Shetti: Validation, Methodology, Advisor, Technical support.

Conflict of interest

No potential conflict of interest was reported by the authors.

Data availability

The datasets generated and/or analyzed during the current study are available from the corresponding author on reasonable request.

Funding

This work was supported by the Department of Chemistry, National Institute of Technology Karnataka, Surathkal, Mangalore India.

References

[1] Jurczynski, Y., Passos, R., & Campos, L. C. (2024). A review of the most concerning chemical contaminants in drinking water for human health. *Sustainability*, *16*, 7107.

[2] Fang, Z., Li, Y., Huang, C., & Liu, Q. (2023). Amine functionalization of iron-based metal-organic frameworks MIL-101 for removal of arsenic species: Enhanced adsorption and mechanisms. *Journal of Environmental Chemical Engineering*, *11*, 110155. https://doi.org/10.1016/j.jece.2023.110155

[3] Kumar, M., Isloor, A. M., Rao, T. S., Ismail, A. F., Farnood, R., & Nambissan, P. (2020). Removal of toxic arsenic from aqueous media using polyphenylsulfone/cellulose acetate hollow fiber membranes containing zirconium oxide. *Chemical Engineering Journal*, *393*, 124367. https://doi.org/10.1016/j.cej.2020.124367

[4] Anand, V., Kaur, J., Srivastava, S., Bist, V., Singh, P., & Srivastava, S. (2022).

Arsenotrophy: A pragmatic approach for arsenic bioremediation. *Journal of Environmental Chemical Engineering*, *10*, 107528. https://doi.org/10.1016/j.jece.2022.107528

[5] Prabhakar, N., Isloor, A. M., Padaki, M., & Fauzi Ismail, A. (2024). Fabrication of TiO2@ZIF-67 metal organic framework composite incorporated PVDF membranes for the removal of hazardous reactive black 5 and Congo red dyes from contaminated water. *Chemical Engineering Journal*, *498*, 155270. https://doi.org/10.1016/j.cej.2024.155270

[6] Satishkumar, P., Isloor, A. M., Rao, L. N., & Farnood, R. (2024). Fabrication of 2D vanadium MXene polyphenylsulfone ultrafiltration membrane for enhancing the water flux and for effective separation of humic acid and dyes from wastewater. *ACS Omega*, *9*, 25766–25778. https://doi.org/10.1021/acsomega.3c10078

[7] Prabhakar, R., & Samadder, S. (2018). Low cost and easy synthesis of aluminium oxide nanoparticles for arsenite removal from groundwater: A complete batch study. *Journal of Molecular Liquids*, *250*, 192–201. https://doi.org/10.1016/j.molliq.2017.11.173

[8] Schaep, J., Vandecasteele, C., Peeters, B., Luyten, J., Dotremont, C., & Roels, D. (1999). Characteristics and retention properties of a mesoporous γ-Al_2O_3 membrane for nanofiltration. *Journal of Membrane Science*, *163*, 229–237. https://doi.org/10.1016/S0376-7388(99)00163-5

[9] Garcia-Ivars, J., Alcaina-Miranda, M.-I., Iborra-Clar, M.-I., Mendoza-Roca, J.-A., & Pastor-Alcañiz, L. (2014). Enhancement in hydrophilicity of different polymer phase-inversion ultrafiltration membranes by introducing PEG/Al_2O_3 nanoparticles. *Separation and Purification Technology*, *128*, 45–57. https://doi.org/10.1016/j.seppur.2014.03.012

[10] Siddique, T., Balu, R., Mata, J., Dutta, N. K., & Roy Choudhury, N. (2022). Electrospun composite nanofiltration membranes for arsenic removal. *Polymers*, *14*, 1980.

[11] Talukder, M. E., Pervez, M. N., Jianming, W., Stylios, G. K., Hassan, M. M., Song, H., Naddeo, V., & Figoli, A. (2022). Ag nanoparticles immobilized sulfonated polyethersulfone/polyethersulfone electrospun nanofiber membrane for the removal of heavy metals. *Scientific Reports*, *12*, 5814.

[12] Kumar, M., Isloor, A. M., Todeti, S. R., Nagaraja, H. S., Ismail, A. F., & Susanti, R. (2021). Effect of binary zinc-magnesium oxides on polyphenylsulfone/cellulose acetate derivatives hollow fiber membranes for the decontamination of arsenic from drinking water. *Chemical Engineering Journal*, *405*, 126809. https://doi.org/10.1016/j.cej.2020.126809

[13] He, J., Matsuura, T., & Chen, J. P. (2014). A novel Zr-based nanoparticle-embedded PSF blend hollow fiber membrane for treatment of arsenate contaminated water: Material development, adsorption and filtration studies, and characterization. *Journal of Membrane Science*, *452*, 433–445. https://doi.org/10.1016/j.memsci.2013.10.041

[14] Potla Durthi, C., Rajulapati, S. B., Palliparambi, A. A., Kola, A. K., & Sonawane, S. H. (2018). Studies on removal of arsenic using cellulose acetate–zinc oxide nanoparticle mixed matrix membrane. *International Nano Letters*, *8*, 201–211. https://doi.org/10.1007/s40089-018-0245-3

[15] Kajekar, A. J., Dodamani, B. M., Isloor, A. M., Karim, Z. A., Cheer, N. B., Ismail, A. F., & Shilton, S. J. (2015). Preparation and characterization of novel PSf/PVP/PANI-nanofiber nanocomposite hollow fiber ultrafiltration membranes and their possible applications for hazardous dye rejection. *Desalination*, *365*, 117–125. https://doi.org/10.1016/j.desal.2015.02.028

[16] Hebbar, R. S., Isloor, A. M., Ananda, K., Abdullah, M. S., & Ismail, A. F. (2017). Fabrication of a novel hollow fiber membrane decorated with functionalized Fe2O3 nanoparticles: Towards sustainable water treatment and biofouling control. *New Journal of Chemistry*, *41*, 4197–4211. https://doi.org/10.1039/C7NJ00221A

[17] Kumar, M., RaoT, S., Isloor, A. M., Ibrahim, G. S., Ismail, N., Ismail, A. F., & Asiri, A. M. (2019). Use of cellulose acetate/polyphenylsulfone derivatives to fabricate ultrafiltration hollow

fiber membranes for the removal of arsenic from drinking water. *International Journal of Biological Macromolecules*, *129*, 715–727. https://doi.org/10.1016/j.ijbiomac.2019.02.017

[18] Vijesh, A. M., Shyma, P. C., Prakash, V., & Garudachari, B. (2018). Preparation and characterization of polysulfone based hollow fibre composite membranes for water purification. *Journal of Applied Membrane Science & Technology*, *22*(2), 109–118. https://doi.org/10.11113/amst.v22n2.130

[19] Nayak, S. S., Isloor, A. M., & Ismail, A. (2025). chicken egg white-based amyloid–graphitic carbon nitride composite-incorporated hollow fiber membrane for efficient removal of dyes and heavy metal ions present in water. *Journal of Materials Chemistry A,* 13, 31304-31318 https://doi.org/10.1039/D5TA02761F

[20] Krause, B., Storr, M., & Zweigart, C. (2017). Membrane innovation in dialysis. *Expanded Hemodialysis: Innovative Clinical Approach in Dialysis*, *191*, 100–114.

[21] Moideen K, I., Isloor, A. M., Ismail, A. F., Obaid, A., & Fun, H. K. (2015). Fabrication and characterization of new PSF/PPSU UF blend membrane for heavy metal rejection. *Desalination and Water Treatment*, *57*, 19810–19819. https://doi.org/10.1080/19443994.2015.1106985

[22] Syed Ibrahim, G. P., Isloor, A. M., Ismail, A. F., & Farnood, R. (2020). One-step synthesis of zwitterionic graphene oxide nanohybrid: Application to polysulfone tight ultrafiltration hollow fiber membrane. *Scientific Reports*, *10*, 1–13. https://doi.org/10.1038/s41598-020-63356-2

[23] Dhawale, V. P., Khobragade, V., & Kulkarni, S. D. (2018). Synthesis and characterization of aluminium oxide (Al_2O_3) nanoparticles and its application in azodye decolourisation. *Chemistry*, *27*, 31. https://doi.org/10.11648/j.ijec.20180201.13

[24] Ali, S., Abbas, Y., Zuhra, Z., & Butler, I. S. (2019). Synthesis of γ-alumina (Al_2O_3) nanoparticles and their potential for use as an adsorbent in the removal of methylene blue dye from industrial wastewater. *Nanoscale Advances*, *1*, 213–218. https://doi.org/10.1039/C8NA00014J

[25] Nethravathi, Isloor, A. M., & Kumar, S. M. (2024). Ion exchange membranes in reverse electrodialysis process. In A. Basile & K. Ghasemzadeh (Eds.), *Current trends and future developments on (bio-) membranes* (pp. 157–189). Elsevier. https://doi.org/10.1016/B978-0-323-88509-6.00007-1

[26] Karunakaran, G., Suriyaprabha, R., Rajendran, V., & Kannan, N. (2015). Effect of contact angle, zeta potential and particles size on the in vitro studies of Al_2O_3 and SiO_2 nanoparticles. *IET Nanobiotechnology*, *9*, 27–34.

[27] Liu, D., Pourrahimi, A. M., Olsson, R. T., Hedenqvist, M. S., & Gedde, U. W. (2015). Influence of nanoparticle surface treatment on particle dispersion and interfacial adhesion in low-density polyethylene/aluminium oxide nanocomposites. *European Polymer Journal*, *66*, 67–77. https://doi.org/10.1016/j.eurpolymj.2015.01.046

[28] Wang, Z. G., Jing, M., Yao, T. T., & Liu, K. G. (2013). SEM image and EDS composition analysis of Al_2O_3 power under low vacuum level condition. *Advanced Materials Research*, *820*, 92–96. https://doi.org/10.4028/www.scientific.net/AMR.820.92

[29] Zhang, X. Z., Zhou, J. E., Jiang, Y. H., & Zhang, J. (2012). Preparation of highly permeable Al_2O_3 hollow fiber membrane via phase inversion method with ethanol as external coagulant. *Advanced Materials Research*, *412*, 203–206. https://doi.org/10.4028/www.scientific.net/AMR.412.203

[30] Feng, H., Wang, H., Ma, Z., Wang, S., & Li, P. (2022). Quantification of surface orientation effect on the thermal stability of γ-Al_2O_3 with different morphologies. *Applied Surface Science*, *594*, 153509. https://doi.org/10.1016/j.apsusc.2022.153509

[31] Wei, M., Zhang, Y., Wang, Y., Liu, X., Li, X., & Zheng, X. (2024). Employing atomic force microscopy (AFM) for microscale investigation of interfaces and interactions in membrane fouling processes: New perspectives and prospects. *Membranes*, *14*, 35.

[32] Ghosh, S., Prabhakar, R., & Samadder, S. (2019). Performance of γ-aluminium oxide nanoparticles for arsenic removal from groundwater. *Clean Technologies and Environmental Policy*, *21*, 121–138. https://doi.org/10.1007/s10098-018-1622-3

[33] Geng, S., Chen, D., Guo, Z., Li, Q., Wen, M., Wang, J., Guo, K., Wang, J., Wang, Y., & Yu, L. (2025). Halloysite-nanotube-mediated high-flux γ-Al_2O_3 ultrafiltration membranes for semiconductor wastewater treatment. *Membranes*, *15*, 130.

[34] Etemadi, H., & Qazvini, H. (2021). Investigation of alumina nanoparticles role on the critical flux and performance of polyvinyl chloride membrane in a submerged membrane system for the removal of humic acid. *Polymer Bulletin*, *78*, 2645–2662. https://doi.org/10.1007/s00289-020-03234-z

[35] Taghavian, H., Černík, M., & Dvořák, L. (2023). Advanced (bio)fouling resistant surface modification of PTFE hollow-fiber membranes for water treatment. *Scientific Reports*, *13*, 11871.

[36] Sherugar, P., Naik, N. S., Padaki, M., Nayak, V., Gangadharan, A., Nadig, A. R., & Déon, S. (2021). Fabrication of zinc doped aluminium oxide/polysulfone mixed matrix membranes for enhanced antifouling property and heavy metal removal. *Chemosphere*, *275*, 130024. https://doi.org/10.1016/j.chemosphere.2021.130024

[37] Adam, M. R., Hubadillah, S. K., Esham, M. I. M., Othman, M. H. D., Rahman, M. A., Ismail, A. F., & Jaafar, J. (2019). Adsorptive membranes for heavy metals removal from water. In *Membrane separation principles and applications* (pp. 361–400). Elsevier. https://doi.org/10.1016/B978-0-12-812815-2.00012-0

[38] Jang, Y., Kim, S. S., & Nguyen, D. D. (2025). Advanced TiO2 and Al_2O_3 modularized adsorbents and practical application strategies for enhanced arsenic removal from water. *Water, Air, & Soil Pollution*, *236*, 469. https://doi.org/10.1007/s11270-025-08094-9

[39] Hamid, N. H. A., Rushdan, A. I., Nordin, A. H., Faiz Norrrahim, M. N., Muhamad, S. N. H., Tahir, M. I. H. M., Rosli, N. S. B., Pakrudin, N. H. M., Roslee, A. S., & Asyraf, M. R. M. (2024). A review: The state-of-the-art of arsenic removal in wastewater. *Water Reuse*, *14*, 279–311.

[40] Marino, T., Russo, F., Rezzouk, L., Bouzid, A., & Figoli, A. (2017). PES-kaolin mixed matrix membranes for arsenic removal from water. *Membranes*, *7*, 57.

How to cite this paper:

Isloor, A. M., Dasaiah, M. S., Venkatesh, M. & Shetti, V. (2026). Enhanced arsenic (V) removal from water using aluminium oxide nanoparticle-incorporated Polyethersulfone hollow fiber membranes. Advances in Environmental Technology, 12(2), 220-231. DOI: 10.22104/aet.2026.7907.2213